PET Evaluation of Novel Radiofluorinated Reboxetine Analogs as Norepinephrine Transporter Probes in the Monkey Brain

MAGNUS SCHOU,[1] CHRISTER HALLDIN,[1*] JUDIT SÓVÁGÓ,[1] VICTOR W. PIKE,[2] HÅKAN HALL,[1] BALÁZS GULYÁS,[1] P. DAVID MOZLEY,[3] DAVID DOBSON,[3] E. SHCHUKIN,[1] ROBERT B. INNIS,[2] AND LARS FARDE[1]

[1]*Karolinska Institutet, Department of Clinical Neuroscience, Psychiatry Section, Karolinska Hospital, S-17176 Stockholm, Sweden*
[2]*Molecular Imaging Branch, National Institute of Mental Health, National Institutes of Health, Bethesda, Maryland 20892*
[3]*Eli Lilly Co, Indianapolis, Indiana 46285*

ABSTRACT   (S,S)-2-(α-(2-Fluoromethoxyphenoxy)benzyl)morpholine ((S,S)-FMeNER) was found to be a selective high-affinity ligand for the norepinephrine transporter (NET). (S,S)-FMeNER) was labeled with fluorine-18 ($t_{1/2}$ = 109.8 min) by *O*-fluoromethylation of desfluoromethoxy-(S,S)-FMeNER with [^{18}F]bromofluoromethane. An analog, *di*-deuterated in the fluoromethoxy group ((S,S)-FMeNER-D$_2$), was similarly labeled with *di*-deutero-[^{18}F]bromofluoromethane. These two new radioligands were obtained in radiochemical purities greater than 98% and with specific radioactivities ranging from 111–185 GBq/µmol at the end of synthesis (75 min). After intravenous injection of (S,S)-[^{18}F]FMeNER into cynomolgus monkey, PET examination with the head in the field of view revealed skull-bound radioactivity, contaminating images of the brain, and indicated fast defluorination of the radioligand. Defluorination was much reduced in similar PET experiments with (S,S)-[^{18}F]FMeNER-D$_2$. Ratios of radioactivity in the lower brainstem, mesencephalon, thalamus, and temporal cortex to striatum obtained with (S,S)-[^{18}F]FMeNER-D$_2$ at 160 min after i.v. injection were 1.5, 1.6, 1.3, and 1.5, respectively. In another PET experiment, pretreatment of the monkey with the selective NET inhibitor, desipramine, decreased the radioactivity ratios in all examined regions to near unity (e.g., to a ratio of 1.03 in mesencephalon). Labeled metabolites of (S,S)-[^{18}F]FMeNER-D$_2$ or (S,S)-[^{18}F]FMeNER found in plasma were all more polar than the parent radioligand. In vitro autoradiography of (S,S)-[^{18}F]FMeNER-D$_2$ on post-mortem human brain cryosections furthermore showed specific binding to NET in the locus coeruleus and thalamus. (S,S)-[^{18}F]FMeNER-D$_2$ is the first useful radiofluorinated ligand for imaging brain NET in monkey in vivo and is superior to (S,S)-[^{11}C]MeNER because a specific binding peak equilibrium is obtained during the PET experiment at a lower noise level. **Synapse 53:57–67, 2004.**   © 2004 Wiley-Liss, Inc.

INTRODUCTION

The norepinephrine transporter (NET) is of interest in the pathophysiology of several neuropsychiatric and neurodegenerative disorders (Brunello et al., 2002; Klimek et al., 1997; Tejani-Butt et al., 1993) and an established target in the treatment of mood disorders and ADHD (Spencer et al., 2002). To better understand the role of NET, research would benefit from methods allowing quantitative mapping of NETs in the living human brain by using positron emission tomography (PET). A previous evaluation of a carbon-11 ($t_{1/2}$ = 20.4 min) labelled *O*-methyl reboxetine analog, (S,S)-[^{11}C]MeNER ([^{11}C]**1**, Fig. 1), has shown that the spe-

cific binding to NET increased continuously towards the end of a PET measurement (90 min from injection) and did not reach specific binding peak equilibrium during the PET measurement (Schou et al., 2003). This, together with a somewhat noisy final signal,
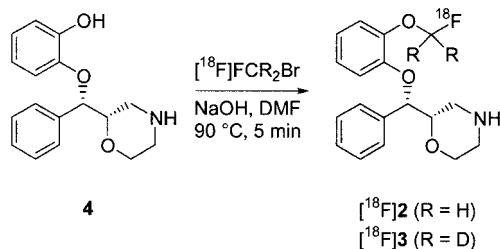
Scheme 1.   Labeling of (S,S)-FMeNER (2) and (S,S)-FMeNER-D$_2$ (3).

Fig. 1.   Structures of (S,S)-MeNER (**1**), (S,S)-FMeNER (**2**), (S,S)-FMeNER-D$_2$ (**3**).

might provide problems for quantitative studies of NET in brain using (S,S)-[^{11}C]MeNER.

As the specific binding of (S,S)-[^{11}C]MeNER increases continuously with time, it is of interest to extend the time of data acquisition by introducing a longer-lived fluorine-18 ($t_{1/2}$ = 109.8 min) label into the ligand. We assumed that the NET-binding characteristics and pharmacokinetics of a radiofluorinated analog would not be too different from those of (S,S)-MeNER, since F for H replacement in the methoxy group may not cause great changes in important properties (e.g., molecular weight, molecular shape, and lipophilicity).

(S,S)-MeNER contains an aryl methoxy group that is attractive to replace with a fluoromethoxy group. Radioligands containing ^{18}F-labeled aryl fluoromethyl ethers have recently been developed, such as the serotonin transporter (SERT) radioligand (+)-[^{18}F]FMcN5652 (thioether) (Marjamaki et al., 2003) and the NK-1 receptor radioligand [^{18}F]SPA-RQ (Hargreaves, 2002). A study with a di-deuterated analog of the latter compound ([^{18}F]DSPA-RQ) has also demonstrated that the in vivo defluorination rate of aryl fluoromethoxy compounds can be reduced through a deuterium isotope effect (Hamill et al., 2002). This observation is of particular importance in PET studies in non-human primates, for which defluorination rates have been reported to be faster than in human subjects (Hamill et al., 2002).

On this basis, in this study we aimed to prepare (S,S)-[^{18}F]FMeNER ([^{18}F]**2**, Fig. 1) and also (S,S)-[^{18}F]FMeNER-D$_2$ ([^{18}F]**3**, Fig. 1), the *di*-deuterated analog, as prospective PET radioligands for NET. The radioligands were evaluated in preliminary studies in cynomolgus monkey.

In a preliminary pharmacological assay (S,S)-FMeNER-D$_2$ was found to be almost equipotent to (S,S)-MeNER (K$_i$ = 3.1 vs. 2.5 nM at NET) and selective over the other two major monoamine transporters (K$_i$'s at SERT and DAT >1,000 nM) (Eli Lilly Co., Indianapolis, IN, data on file).

MATERIALS AND METHODS
Materials

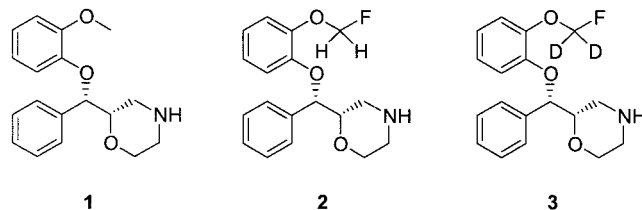N,N-Dimethylformamide (DMF) was obtained from Merck (Darmstadt, Germany), distilled under vacuum, and dried over molecular sieves (4 Å). The precursor, NER (Nor-Ethyl-Reboxetine), and standards ((S,S)-FMeNER and (S,S)-FMeNER-D$_2$) were obtained from Eli Lilly Co. Solid phase extraction columns (Sep-Pak light QMA and Sep-Pak Plus Silica) were obtained from Waters Instruments (Rochester, MN). Dry acetonitrile (MeCN, max 10 ppm H$_2$O) was obtained from Merck. Dibromomethane and dibromomethane-d_2 were obtained from Aldrich (Milwaukee, WI). Other chemicals were obtained from commercial sources and were of analytical grade and used without further purification.

[^{18}F]Fluoride was produced at the Karolinska Hospital with a GEMS PETtrace cyclotron using 16 MeV protons in the ^{18}O(p,n) ^{18}F reaction on ^{18}enriched water (10–95%).

General methods

Radioligands, (S,S)-[^{18}F]FMeNER and (S,S)-[^{18}F]FMeNER-D$_2$, were each purified by reverse-phase HPLC on a µ-Bondapak C-18 column (300 × 7.8 mm, 10 µm; Waters Instruments) eluted with MeCN-NH$_4$OCHO (0.1 M) (30:70 v/v) at 6 mL/min (system A). Eluate was monitored with a UV absorbance detector (λ = 254 nm) in series with a GM-tube for radioactivity detection. The radiochemical purity of each radioligand was determined by reverse phase HPLC on a µ-Bondapak C-18 column (300 × 3.9 mm; 10 µm; Waters Instruments) eluted with MeCN-H$_3$PO$_4$ (10 mM) (30:70 v/v) at 2 mL/min (system B). Eluate was monitored with a UV absorbance detector (λ = 254 nm) in series with a radioactivity detector (β-flow; Beckman, Fullerton, CA). (S,S)-[^{18}F]FMeNER and (S,S)-[^{18}F]FMeNER-D$_2$ were identified by co-injection with non-labeled standards.

The stability of radioligands was tested with HPLC (system B) and TLC on silica gel (CH$_2$Cl$_2$-MeOH-H$_2$O; 10:2.5:0.1 by vol.). TLC plates were scanned with an AR-2000 Imaging Scanner (Bioscan Inc., Washington, DC) and analyzed with the Winscan 2.2 software (LabLogic Inc., Sheffield, UK) The Rf values of (S,S)-FMeNER and (S,S)-FMeNER-D$_2$ were between 0.2 and 0.3.
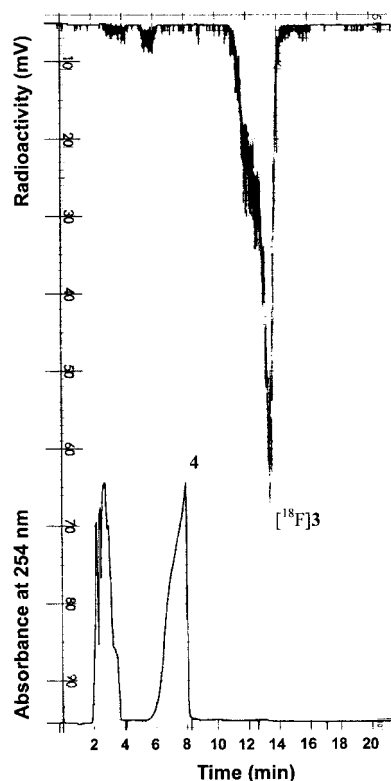
Fig. 2. HPLC chromatogram from the separation of [18F](*S,S*)-FMeNER-D$_2$. The injection was made at approximately 1 min. See text for HPLC conditions.

Radiochemistry

[18F]Bromofluoromethane

[18F]Bromofluoromethane was prepared from [18F]fluoride ion by adapting a described method (Iwata et al., 2002). Thus, a solution of [18F]fluoride ion in [18]enriched water was flushed through a preconditioned (K$_2$CO$_3$ [0.5 M], 10 mL), 18 MΩ H$_2$O, 15 mL) Sep-Pak QMA light cartridge to isolate [18F]fluoride ion. [18F]Fluoride ion was then eluted from the cartridge with a solution of K$_2$CO$_3$ (7 μmol), Kryptofix 2.2.2 (130 μmol) in water (18 MΩ, 43 μL) and MeCN (2 mL). Solvents were evaporated off at 170°C under nitrogen flow, leaving a yellow residue. The residue was cooled to room temperature (RT) and then dibromomethane (50 μL) in MeCN (1 mL) added. The reaction vessel was then heated to 90°C while vented through three silica Sep-Paks linked in series. Heating was continued until a rapid reduction of radioactivity in the reaction vessel ceased (after 10–15 min), after which nitrogen was passed through the reaction vessel to carry volatile products through the Silica Sep-Paks. [18F]Bromofluoromethane was trapped from the effluent in DMF (400 μL) at 0°C.

[18F]Bromofluoromethane-*d₂*

[18F]Bromofluoromethane-*d₂* was prepared according to the method described for [18F]bromofluoromethane, except that dibromomethane-*d₂* replaced dibromomethane.
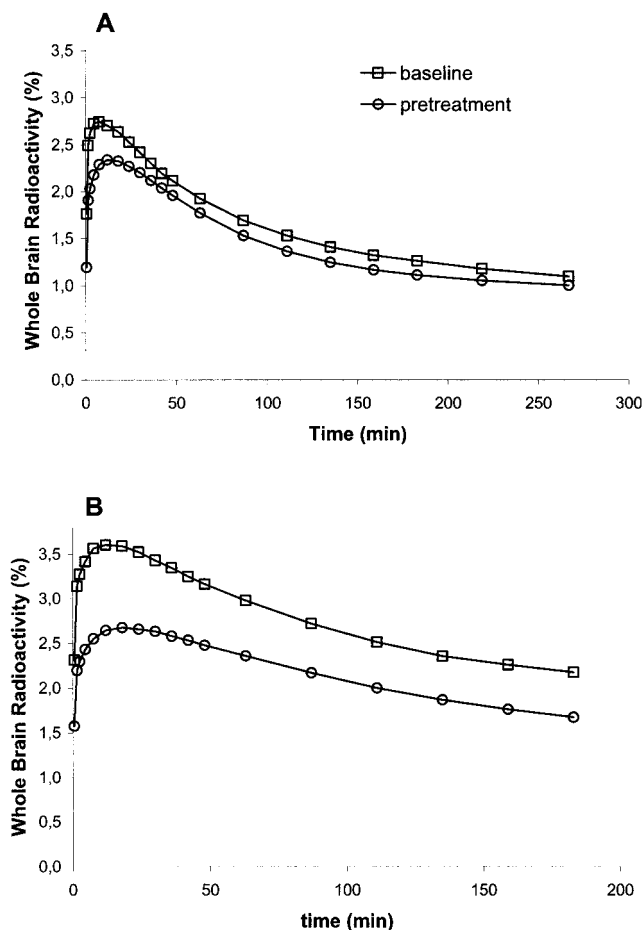

Fig. 3. Whole brain uptake as percentage of injected radioactivity at baseline and pre-treatment conditions (DMI 5 mg/kg) with (*S,S*)-[18F]FMeNER (**A**) and (*S,S*)-[18F]FMeNER -D$_2$ (**B**).

[18F]Fluoromethyl triflate

[18F]Fluoromethyl triflate was prepared by sweeping [18F]bromofluoromethane through a heated glass column containing silver triflate impregnated on graphitised carbon (Iwata et al., 2002).

[18F]Fluoromethyl-*d₂* triflate

[18F]fluoromethyl-*d₂* triflate was prepared according to the method decribed for [18F]fluoromethyl triflate, except that dibromomethane-*d₂* replaced dibromomethane.

(S,S)-[18F]FMeNER ([18F]2)

To a solution of [18F]bromofluoromethane in DMF (400 μL) was added a mixture of phenol **4** (1 mg, 3.5 μmol) and sodium hydroxide (5M, 6 μL) in DMF (200 μL). The vessel was sealed and heated at 90°C for 5 min. HPLC mobile phase (400 μL) was added to the
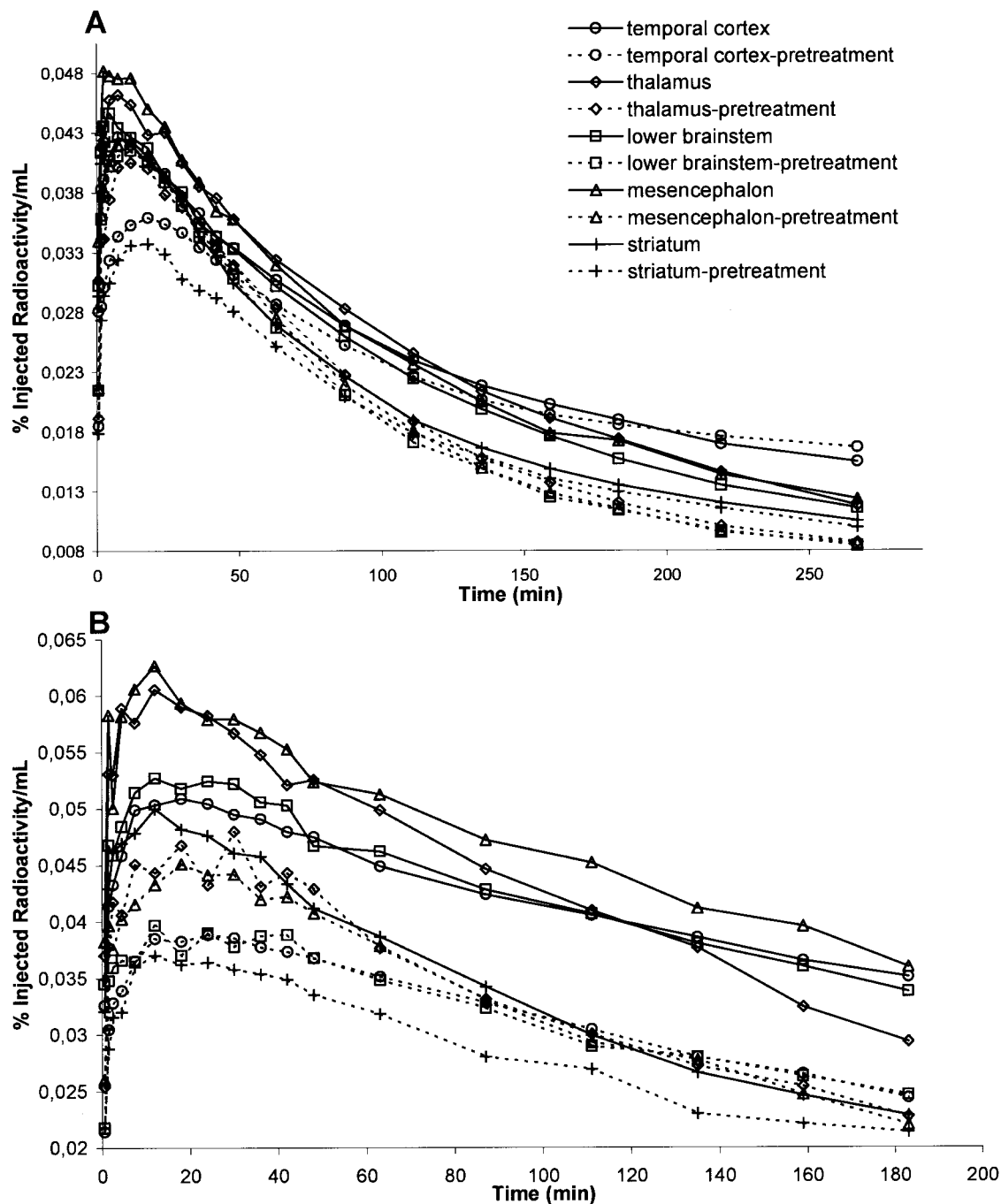
Fig. 4. Time-radioactivity curves obtained after i.v. injection of (S,S)-[18F]FMeNER (A,C) and (S,S)-[18F]FMeNER-D$_2$ (B,D). **A:** Regional radioactivity distribution following i.v. injection of (S,S)-[18F]FMeNER during baseline (solid lines) and pre-treatment conditions (DMI 5 mg/kg, dotted lines). **B:** Regional radioactivity distribution following i.v. injection of (S,S)-[18F]FMeNER-D$_2$ during baseline (solid lines) and pre-treatment conditions (DMI 5 mg/kg, dotted lines). **C:** Specific binding of (S,S)-[18F]FMeNER during baseline experiment. **D:** Specific binding of (S,S)-[18F]FMeNER-D$_2$ during baseline experiment.

crude reaction mixture before its injection onto HPLC (System A). The fraction eluting with a retention time of 12–13 min (Fig. 2) was evaporated to dryness. The residue was dissolved in sterile disodium phosphate buffered saline (PBS; pH 7.4; 8 mL) and filtered through a sterile filter (0.22 μm; Millipore, Bedford,

MA), yielding a sterile and apyrogenic solution of [18F]**2**.

(S,S)-[18F]FMeNER-D$_2$ ([18F]3)

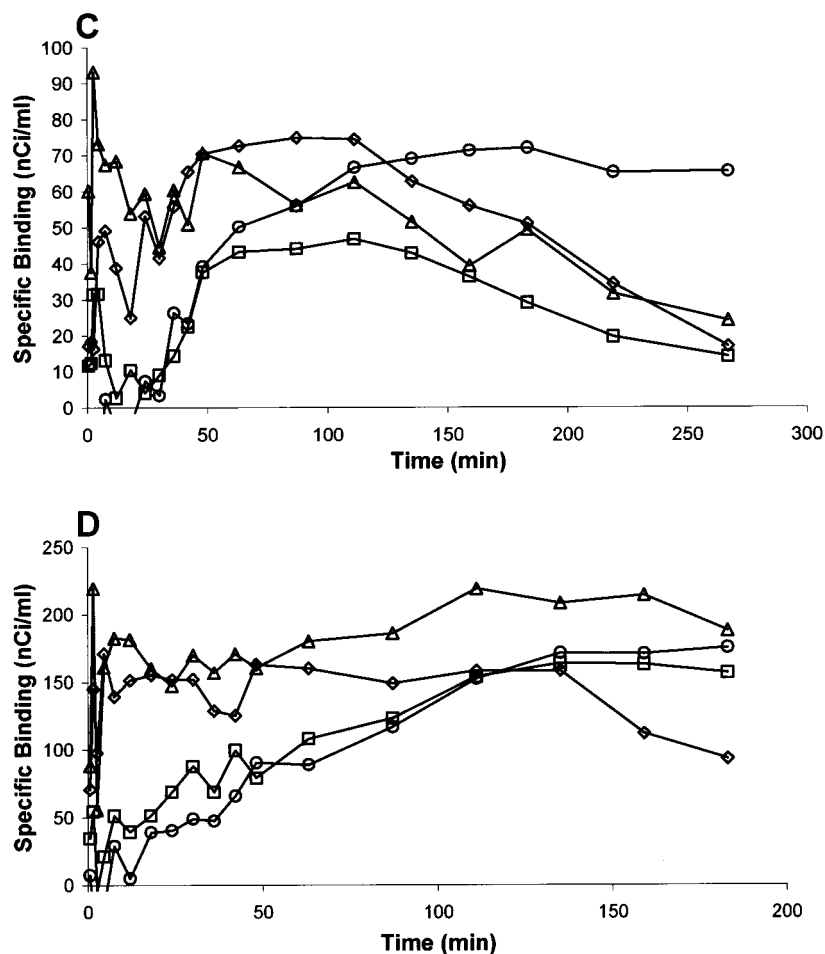(S,S)-[18F]FMeNER-D$_2$ ([18F]**3**) was prepared according the method described for [18F]**2** except that

Figure 4 (Continued.)

[18F]bromofluoromethane-d_2 replaced [18F]bromofluoromethane.

Alternative method for preparation of (S,S)-[18F]FMeNER and (S,S)-[18F]FMeNER-D$_2$

[18F]Fluoromethyl or [18F]fluoromethyl-d_2 triflate was trapped in a vessel containing the *N*-Boc protected precursor (0.5 mg, 1.3 μmol) and aqueous sodium hydroxide (2 μL, 0.5M). After completed trapping, TFA (90 μL) was added and the resulting mixture was heated at 90°C for 4 min to yield crude (S,S)-[18F]FMeNER or (S,S)-[18F]FMeNER-D$_2$.

PET experimental procedure

Two female cynomolgus monkeys (5,150 and 6,995 g) were supplied by the National Institute for Infectious Disease Control, Solna, Stockholm. The study was approved by the Animal Ethics Committee of Northern Stockholm. Anaesthesia was induced and maintained by repeated intramuscular injection of a mixture of ketamine (3–4 mg/kg per h Ketalar®, Parke-Davis) and xylazine hydrochloride (1–2 mg/kg per h Rompun® vet., Bayer, Sweden). A device was used to fix the position of the monkey head during the PET experiments (Karlsson et al., 1993). Body temperature was controlled by a heating pad with thermostat.

The monkeys were examined with a Siemens (South Iselin, NJ) ECAT EXACT HR PET system, which was run in 3D mode. The spatial resolution was about 3.8 mm FWHM (Wienhard et al., 1994). Images were displayed as 47 sections with a separation of 3.3 mm. In each PET experiment, 49–68 MBq of (S,S)-[18F]FMeNER or (S,S)-[18F]FMeNER-D$_2$ was injected as a bolus into the sural vein. Radioactivity in brain was measured according to a pre-programmed sequence of frames during 183 and 267 min, respectively.

Six PET measurements were performed each on a separate day. In the first monkey, a baseline measurement was performed with (S,S)-[18F]FMeNER followed by a pretreatment experiment in which the selective NET inhibitor, desipramine (DMI, 5 mg/kg) was injected intravenously 20 min before injection of (S,S)-[18F]FMeNER.

In the second monkey, the same procedure was repeated except that the di-deuterated ligand (S,S)-[18F]FMeNER-D$_2$ was injected. Two further pretreat-
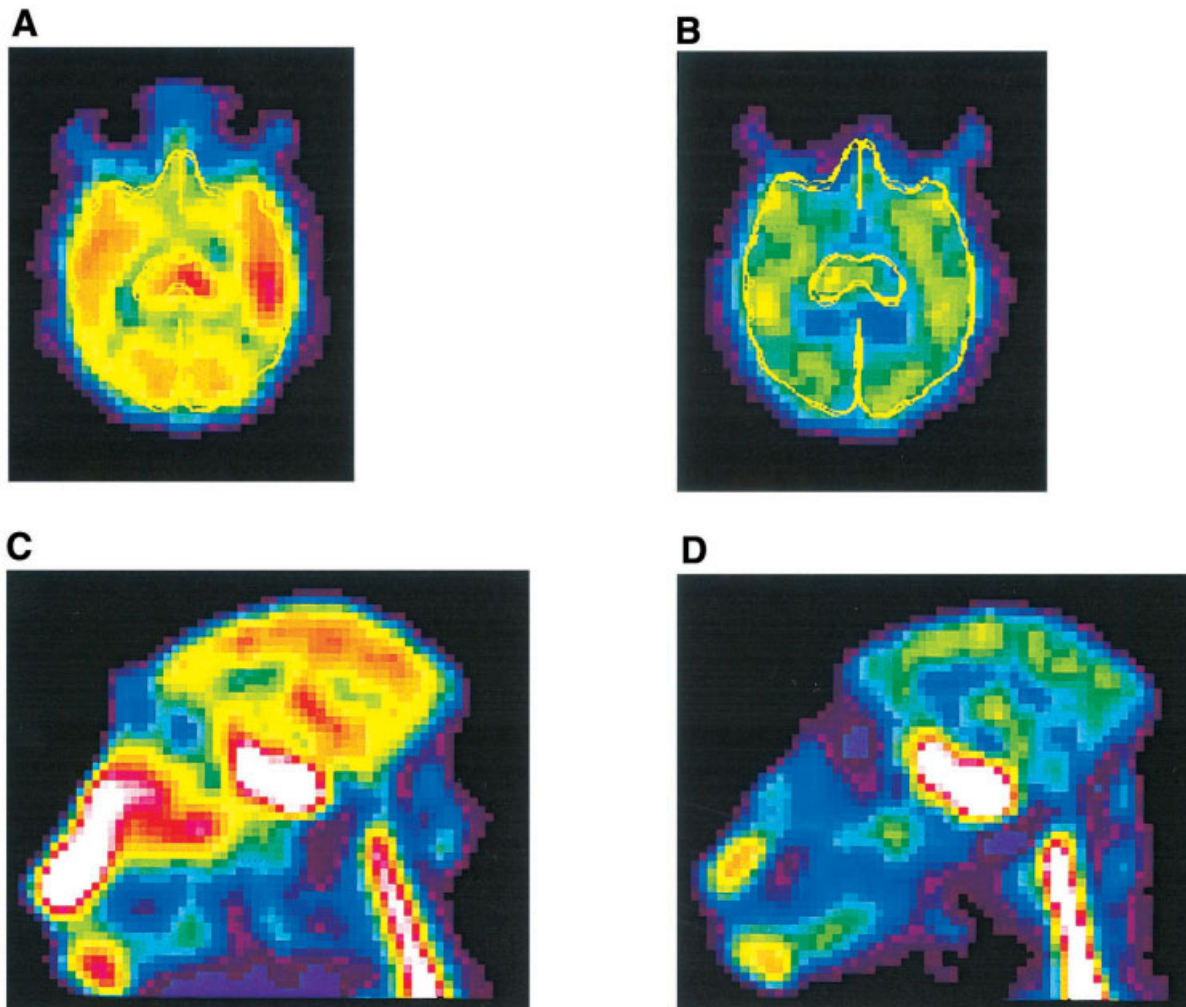
Fig. 5. Color-coded PET images of the Cynomolgus monkey brain obtained after i.v. injection of (S,S)-[^{18}F]FMeNER-D$_2$ during baseline (**A,C**) and pre-treatment (**B,D**) conditions (DMI 5 mg/kg). A and B represent horizontal images. C and D represent saggital images.

ment measurements with (S,S)-[^{18}F]FMeNER-D$_2$ were then performed in the first monkey, the first giving the selective serotonin transporter (SERT) inhibitor, citalopram (5 mg/kg), at 20 min before radioligand injection, and the second giving the reference dopamine transporter (DAT) inhibitor, GBR 12909 (5 mg/kg), at 30 min before radioligand injection.

PET regions of interest

Regions of interest (ROIs) (lower brainstem, mesencephalon, striatum, thalamus, temporal cortex, and whole brain) were drawn on summation images reconstructed for a sum of all frames and were defined according to an atlas of a cryosected Cynomolgus monkey head in situ (Karlsson et al., 1993). The upper arm bone (humerus) was used as a ROI for measurement of bone radioactivity.

Radioactivity was calculated for the sequence of time frames, corrected for radioactive decay, normalized to the injected radioactivity, and plotted versus time. The percent of injected radioactivity present in brain at time of maximal radioactivity concentration (i.e., 8 min after the injection of (S,S)-[^{18}F]FMeNER) was used as an index of drug uptake in the brain. This percentage was calculated by multiplying the brain volume (about 70 mL) with the radioactivity concentration in the ROI for the whole brain divided by the injected radioactivity. The brain volume was calculated by multiplying the sum of the whole brain regions of all PET-sections with the plane separation.

Striatum, which is a region almost devoid of NETs (Charnay et al., 1995; Donnan et al., 1991; Tejani-Butt, 1992) was used as a reference region for the free radioligand concentration and non-specific binding in brain. To calculate specific binding, radioactivity in the striatum was subtracted from the radioactivity in an ROI.
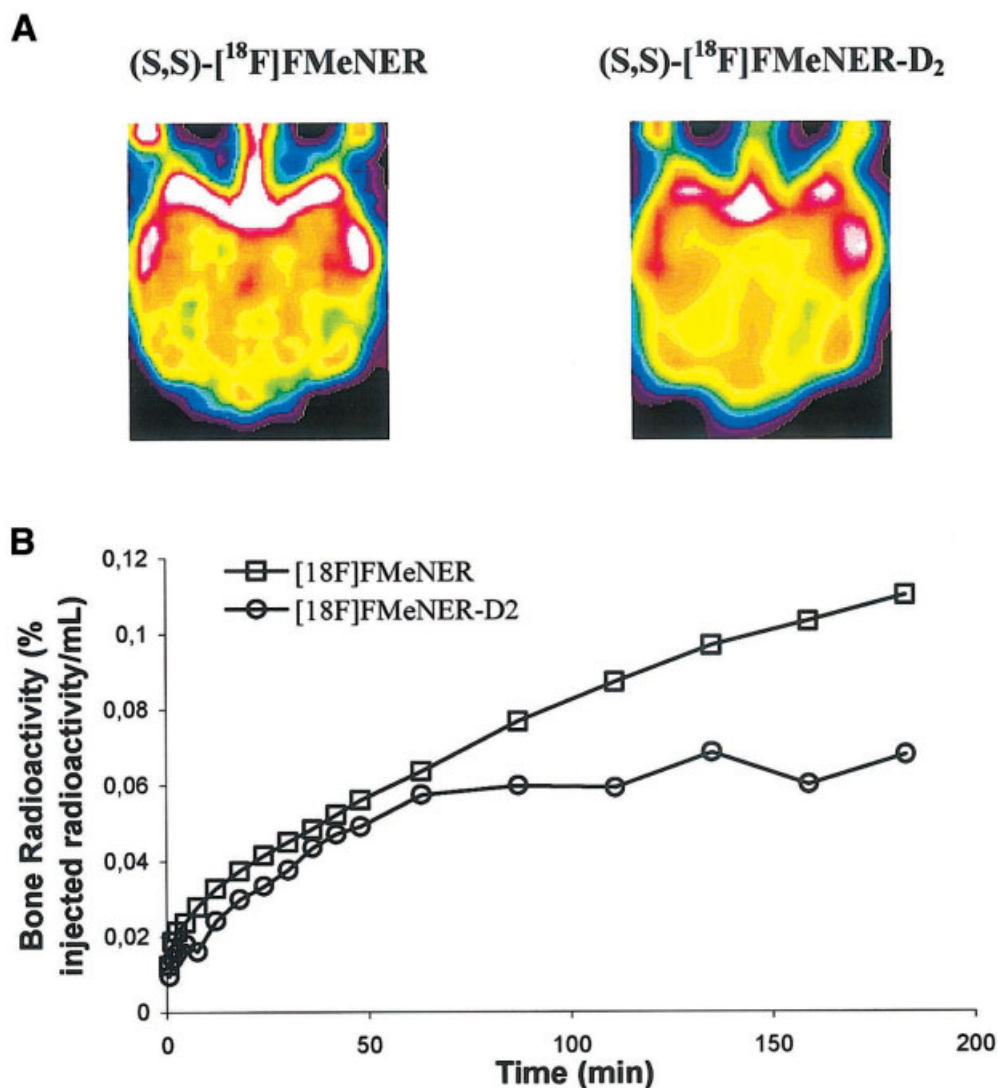
Fig. 6. **A:** Color-coded horizontal PET images of the Cynomolgus monkey brain at the level of mesencephalon obtained after i.v. injection of (S,S)-[^{18}F]FMeNER and (S,S)-[^{18}F]FMeNER-D$_2$. **B:** Radioactivity uptake into the upper arm bone (humerus) following i.v. injection of (S,S)-[^{18}F]FMeNER or (S,S)-[^{18}F]FMeNER-D$_2$.

Plasma metabolite studies and protein binding

The analytical procedure used for determination of the percentages of radioactivity corresponding to unchanged (S,S)-[^{18}F]FMeNER and (S,S)-[^{18}F]FMeNER-D$_2$ and labeled metabolites in monkey plasma was adapted from that reported for other PET radioligands (Halldin et al., 1995). The procedure is also similar to that used for (S,S)-[^{11}C]MeNER (Schou et al., 2003).

Plasma protein binding was determined by ultrafiltration (Halldin et al., 1998). To plasma (~2 mL) was added (S,S)-[^{18}F]FMeNER or (S,S)-FMeNER-D$_2$ (~20 μg). The resulting mixture was then transferred to four Centrisart I (Sartorius AG, Göttingen, Germany) ultrafiltration devices (cutoff at 10,000 Daltons) and the radioactivity in each device was measured. The samples were then incubated for 5 min after which they were centrifuged for 10 min. Total radioactivity and radioactivity in the ultrafiltrate were measured and the amount of free radioligand was calculated by dividing the radioactivity in the ultrafiltrate by the total radioactivity.

In vitro autoradiography

The human brain used was obtained from the National Institute of Forensic Medicine, Karolinska Institutet (Stockholm, Sweden). The brain was removed at clinical autopsy and was handled in a manner similar to that described in detail earlier (Hall et al., 1998). The sections were incubated for 90 min at RT with 4 MBq (S,S)-[^{18}F]FMeNER-D$_2$ in a 50-mM TRIS buffer, pH 7.4, containing 300 mM sodium chloride, 5 mM potassium chloride and 0.1% (w/v) ascorbic acid. The sections were then washed (same buffer) 3 times for 5 min and briefly dipped in cold distilled water before being exposed to Kodak Biomax MR film overnight. Non-specific binding was estimated by simultaneous incubation with DMI (10 μM).

To compare with in vitro results obtained with (*S*,*S*)-[^{11}C]MeNER (Schou et al., 2003), the brain distribution of (*S*,*S*)-[^{18}F]FMeNER-D$_2$ was studied in the same brain and on sections adjacent to those used earlier for (*S*,*S*)-[^{11}C]MeNER.

RESULTS
Radiochemistry

The yield of [^{18}F]bromofluoromethane was between 15–25% (non-corrected) and the subsequent incorporation yield of [^{18}F]bromofluoromethane into (*S*,*S*)-[^{18}F]FMeNER was greater than 90% (measured by analytical HPLC of reaction mixture). The yields of (*S*,*S*)-[^{18}F]FMeNER and (*S*,*S*)-[^{18}F]FMeNER-D$_2$ from [^{18}F]fluoride was between 5–10% with a total synthesis time of about 75 min. The radiochemical purity was better than 98% (t$_R$ 5–5.5 min, system B, flow 2 mL/min). Specific radioactivity at time of injection was about 111–185 GBq/μmol (3,000–5,000 Ci/mmol) corresponding to an injected mass of 0.08–0.2 μg (*S*,*S*)-FMeNER. Radioligands were found to be stable in the PBS formulation for the duration of the experiments. Radiochemical purities were >95% for (*S*,*S*)-[^{18}F]FMeNER or (*S*,*S*)-[^{18}F]FMeNER-D$_2$ at 5 h after formulation, determined by HPLC (system B) and radio-TLC.

(*S*,*S*)-[^{18}F]FMeNER and (*S*,*S*)-[^{18}F]FMeNER-D$_2$ were also obtained from [^{18}F]fluoromethyl or [^{18}F]fluoromethyl-*d*$_2$ triflate in similar incorporation yields as from the [^{18}F]fluoroalkyl halides.

Positron emission tomography

After intravenous injection of (*S*,*S*)-[^{18}F]MeNER at baseline conditions, the maximal radioactivity in the monkey brain was about 2.8% of the total radioactivity at 8 min (Fig. 3A). Of the brain regions examined, the radioactivity was highest in the temporal cortex and lowest in the striatum (Fig. 4A). A specific binding peak equilibrium was obtained at about 90–120 min except in the temporal cortex where the radioactivity increased until about 150 min (Fig. 4C). Ratios of radioactivity at 110 min after injection of (*S*,*S*)-[^{18}F]MeNER in the lower brainstem, mesencephalon, and thalamus to striatum were 1.2, 1.2, and 1.3, respectively. The radioactivity ratio in the temporal cortex to striatum increased to 1.5 at the end of study.

After pretreatment with DMI, the radioactivity in all examined brain regions, except in the temporal cortex, was inhibited to a striatal level (Fig. 4A). The radioactivity ratio in the temporal cortex to striatum increased to 1.7 at the end of the pretreatment study. The total radioactivity in brain was lower (2.3%) in the pretreatment measurement (Fig. 3A) compared to the baseline measurement.

After intravenous injection of (*S*,*S*)-[^{18}F]FMeNER-D$_2$, uptake of radioactivity into brain peaked after 12 min at 3.6 % of the injected radioactivity (Fig. 3B). The
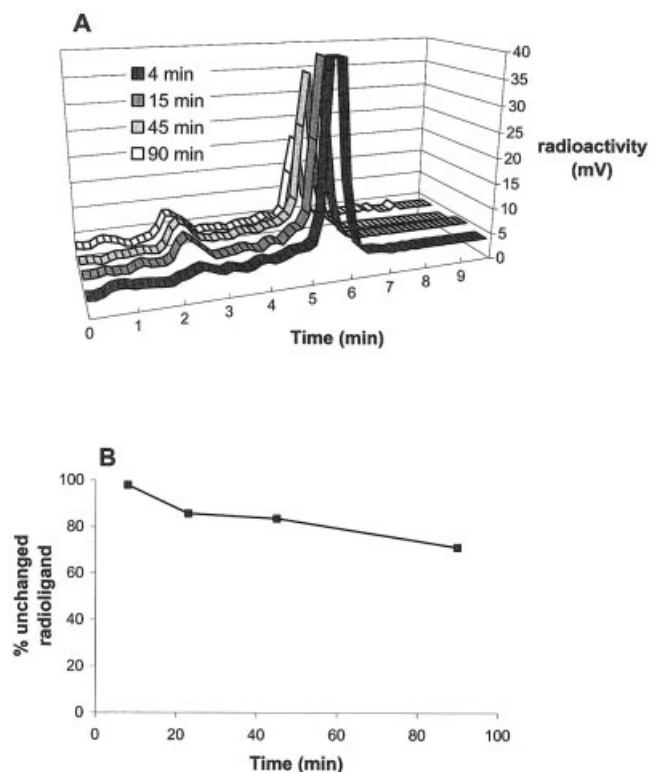

Fig. 7. **A:** Radiochromatograms of samples taken from monkey plasma at 4, 15, 45, and 90 min after i.v. injection of (*S*,*S*)-[^{18}F]FMeNER-D$_2$. **B:** Percent of unchanged (*S*,*S*)-[^{18}F]FMeNER-D$_2$ in plasma from four monkeys.

regional distribution of radioactivity (Figs. 4B, 5A,C) was similar to that in brain after administration of (*S*,*S*)-[^{18}F]FMeNER. The radioactivity in bone reached a plateau at approximately 90 min after injection of (*S*,*S*)-[^{18}F]FMeNER-D$_2$, whereas the bone radioactivity increased throughout the whole experiment after injection of (*S*,*S*)-[^{18}F]FMeNER (Fig. 6). Peak specific binding was found at approximately 120–160 min (Fig. 4C). Ratios of radioactivity in the lower brainstem, mesencephalon, thalamus, and temporal cortex to striatum obtained with (*S*,*S*)-[^{18}F]FMeNER-D$_2$ at 160 min after i.v. injection were 1.5, 1.6, 1.3, and 1.5, respectively.

After pretreatment with DMI, the radioactivity uptake in all examined regions was inhibited (e.g., to a ratio of 1.03 in mesencephalon) (Figs. 4B,D, 5B,D). The radioactivity ratio in the temporal cortex to striatum was 1.2 at 160 min and 1.1 at the end of the pretreatment study.

Interestingly, there was also a conspicuous accumulation of radioactivity in the nasal mucosa, a region known to be rich in NET. The radioactivity in the nasal mucosa was markedly decreased after pre-treatment with DMI (Fig. 5C,D). Pretreatment experiments with GBR 12909 and citalopram did not have any significant effects on the brain distribution of (*S*,*S*)-[^{18}F]FMeNER-D$_2$ (data not shown).
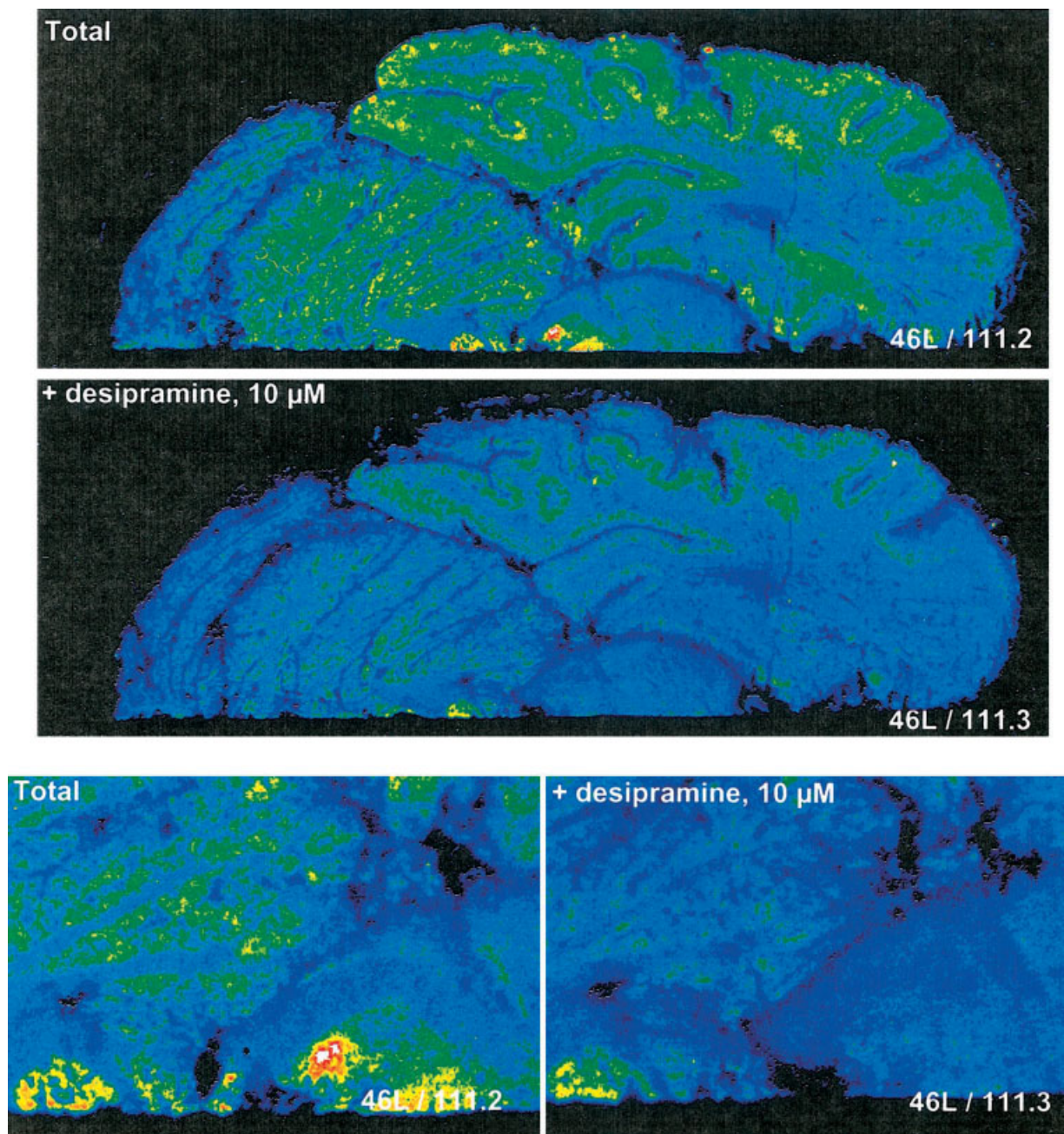
Fig. 8. Whole hemisphere cryosections of the human brain post-mortem incubated with (*S,S*)-[18F]FMeNER-D$_2$ with the region containing the locus coeruleus enlarged (**bottom**). One section was also co-incubated with DMI (10 µM) as indicated.

Plasma metabolite studies

The injected radioactivity eluted in HPLC within 7 min with a good resolution of unchanged radioligand from the labeled metabolites (Fig. 7A). The recovery from the analytical procedure was >95 % (measured at 4-min samples). The labeled metabolites found in monkey plasma after i.v. injection of (*S,S*)-[18F]FMeNER or (*S,S*)-[18F]FMeNER-D$_2$ were more polar than parent radioligand.

The fraction of the total radioactivity in plasma representing unchanged (*S,S*)-[18F]FMeNER or (*S,S*)-[18F]FMeNER-D$_2$ remained high throughout the measurements (Fig. 7B). For (*S,S*)-[18F]FMeNER, it was 82 ± 3 % ($n = 3$) at 45 min after injection. For (*S,S*)-[18F]FMeNER-D$_2$, it was 85 ± 3 % ($n = 4$) at 45 min and 76 ± 6 % ($n = 3$) at 90 min after injection (Fig. 7B).

The free fraction of (*S,S*)-[18F]FMeNER-D$_2$ in plasma determined by ultrafiltration was 22 ± 3 % ($n = 4$).

In vitro autoradiography

(*S,S*)-[^{18}F]FMeNER-D$_2$ bound substantially to cerebral and cerebellar grey matter, showing lower binding to white matter. The binding was most prominent in the locus coeruleus, where it was inhibited by the addition of desipramine (10 μM), indicating specific binding to NET (Fig. 8). Specific binding was also indicated in thalamus (data not shown).

DISCUSSION

No radioligand useful for mapping NETs in the human brain in vivo presently exists. The most promising radioligand reported so far is probably (*S,S*)-[^{11}C]MeNER (Ding et al., 2003; Schou et al., 2003; Wilson et al., 2003). However, this radioligand does not appear to be an ideal radioligand, since a specific binding peak equilibrium was not obtained during a 90-min PET measurement with the radioligand (Schou et al., 2003). From a statistical point of view, it is not optimal to obtain the maximal specific binding at the end of the experiment, when the signal to noise ratios are decreasing due to decay of carbon-11.

Here, we report the preparation and evaluation of two novel radiofluorinated analogs of (*S,S*)-[^{11}C]MeNER, namely (*S,S*)-[^{18}F]FMeNER and (*S,S*)-[^{18}F]FMeNER-D$_2$. The radioligands were obtained in low but sufficient yields to perform the PET measurements. Our aim was to use the radioligands in prolonged PET measurements, in which specific binding peak equilibrium could be obtained.

In the present study, we found that a specific binding peak equilibrium was indeed obtained both after injection of (*S,S*)-[^{18}F]FMeNER and (*S,S*)-[^{18}F]FMeNER-D$_2$. The radioligands had also retained affinity and selectivity for NET after substitution of the methoxy group with a fluoromethoxy group. This was reflected upon the brain distribution of the two radioligands, which was in accordance with reported densities of NETs in the rodent and cat brain (Charnay et al., 1995; Tejani-Butt, 1992). Furthermore, the distribution of radioactivity was also similar to that obtained earlier with (*S,S*)-[^{11}C]MeNER in cynomolgus monkey brain (Schou et al., 2003). Consistent with previously reported data on the metabolic stability of [^{18}F]SPA-RQ (Hamill et al., 2002), a radioligand also containing a fluorine-18 labeled aryl fluoromethoxy ether, the instability of (*S,S*)-[^{18}F]FMeNER towards in vivo defluorination resulted in skull-bound radioactivity that obscured PET imaging of the temporal cortex. Also consistent with the work of Hamill and co-workers (2002), defluorination was diminished by substituting the methylene hydrogens of the fluoromethyl group with deuterium atoms. However, the defluorination was not totally inhibited using this approach and skull-bound radioactivity may thus also contribute to radioactivity in the temporal cortex at baseline PET measurements using

(*S,S*)-[^{18}F]FMeNER-D$_2$, especially as the specific binding peak equilibrium in this region was obtained at a later time-point than in the other examined brain regions.

The approach to introduce deuterons in order to increase the stability of a radioligand has also been used for several other cases, e.g., [^{11}C]L-deprenyl-D$_2$ (Fowler et al., 1995).

(*S,S*)-[^{18}F]FMeNER-D$_2$ specifically labelled NETs in the locus coeruleus in vitro. Further experiments to examine the binding of (*S,S*)-[^{18}F]FMeNER-D$_2$ to human NETs in vitro is currently in progress.

Conclusions

The advantages of (*S,S*)-[^{18}F]FMeNER-D$_2$ over (*S,S*)-[^{11}C]MeNER as a PET radioligand for NET in the monkey brain are that a specific binding peak equilibrium is obtained during the timeframe of a PET study and at a lower noise level.

These results also suggest that (*S,S*)-[^{18}F]FMeNER-D$_2$ may be useful for mapping NETs in the human brain in vitro.

REFERENCES

Brunello NMJ, Kasper S, Leonard B, Montgomery S, Nelson J, Paykel E, Versiani M, Racagni G. 2002. The role of noradrenaline and selective noradrenaline reuptake inhibition in depression. Eur Neuropsychopharmacol 12:461–475.

Charnay Y, Leger L, Vallet P, HOF P, Juovet M, Bouras C. 1995. [^{3}H]Nisoxetine binding sites in the cat brain: an autoradiographic study. Neuroscience 69:259–270.

Ding Y, Lin K, Garza V, Carter P, Alexoff D, Logan J, Shea C, Xu Y, King P. 2003. Evaluation of a new norepinephrine transporter PET ligand in baboons, both in brain and peripheral organs. Synapse 50:345–352.

Donnan G, Kaczmarczyk S, Paxinos G, Chilco P, Kalnins R, Woodhouse D, Mendelsohn F. 1991. Distribution of catecholaminergic uptake sites in human brain as determined by quantitative [^{3}H]mazindol autoradiography. J Comp Neurol 304: 419–434.

Fowler J, Wang G, Logan J, Xie S, Volkow N, MacGregor R, Schlyer D, Pappas N, Alexoff D, Patlak C. 1995. Selective reduction of radiotracer trapping by deuterium substitution: comparison of carbon-11-L-deprenyl and carbon-11-deprenyl-D$_2$ for MAO B mapping. J Nucl Med 36:1255–1262.

Hall H, Halldin C, Farde L, Sedvall G. 1998. Whole hemisphere autoradiography of the postmortem human brain. Nucl Med Biol 25: 715–719.

Halldin C, Swahn C-G, Farde L, Sedvall G. 1995. Radioligand disposition and metabolism. In: Comar D, editor. PET for drug development and evaluation. Dordrecht: Klüwer Academic Publishers. p 55–65.

Halldin C, Foged C, Chou YH, Karlsson P, Swahn CG, Sandell J, Sedvall G, Farde L. 1998. Carbon-11-NNC 112: a radioligand for PET examination of striatal and neocortical D$_1$-dopamine receptors. J Nucl Med 39:2061–2068.

Hamill T, Burns H, Eng W, Ryan C, Krause S, Gibson R, Hargreaves R. 2002. An improved fluorine-18 labeled neurokinin-1 receptor ligand. Mol Imaging Biol 4(Suppl 1):S34.

Hargreaves R. 2002. Imaging substance P receptors (NK1) in the living human brain using positron emission tomography. J Clin Psychiatry 63(Suppl 11):18–24.

Iwata R, Pascali C, Bogni A, Furumoto S, Terasaki K, Yanai K. 2002. [^{18}F]Fluoromethyl triflate, a novel and reactive [^{18}F]fluoromethylating agent: preparation and application to the on-column preparation of [^{18}F]fluorocholine. Appl Radiat Isot 57:347–352.

Karlsson P, Farde L, Halldin C, Swahn C-G, Sedvall G, Foged C, Hansen K, Skrumsager B. 1993. PET examination of [^{11}C]NNC 687 and [^{11}C]NNC 756 as new radioligands for the D1-Dopamine receptor. Psychopharmacology 113:149–156.

Klimek V, Stockmeier C, Overholser J, Meltzer H, Kalka S, Dilley G, Ordway G. 1997. Reduced levels of norepinephrine transporters in the locus coeruleus in major depression. J Neurosci 17:8451–8458.

Marjamaki P, Zessin J, Eskola O, Gronroos T, Haaparanta M, Bergman J, Lehikoinen P, Forsback S, Brust P, Steinbach J, Solin O. 2003. S-[^{18}F]fluoromethyl-(+)-McN5652, a PET tracer for the serotonin transporter: evaluation in rats. Synapse 47:45–53.

Schou M, Halldin C, Sóvágó J, Pike VW, Gulyás B, Mozley P, Johnson D, Hall H, Innis R, Farde L. 2003. Specific in vivo binding to the norepinephrine transporter demonstrated with the PET radioligand, (S,S)-[^{11}C]MeNER. Nucl Med Biol 30:707–714.

Spencer T, Heiligenstein J, Biederman J, Faries D, Kratochvil C, Conners C, Potter W. 2002. Results from 2 proof-of-concept, placebo-controlled studies of atomoxetine in children with attention-deficit/hyperactivity disorder. J Clin Psychiatry 63:1140–1147.

Tejani-Butt S. 1992. [3H]Nisoxetine: A radioligand for quantitation of norepinephrine uptake sites by autoradiography or by homogenate binding. J Pharm Exp Ther 260:427–436.

Tejani-Butt S, Yang J, Zaffar H. 1993. Norepinephrine transporter sites are decreased in the locus coeruleus in Alzheimer's disease. Brain Res 631:147–150.

Wienhard K, Dahlbom M, Eriksson L, Michel C, Bruckbauer T, Pietrzyk U, Heiss W. 1994. The ECAT Exact HR: Performance of a new high resolution positron scanner. J Comput Assist Tomogr 18:110–118.

Wilson A, Johnson D, Mozley P, Hussey D, Ginovart N, Nobrega J, Garcia A, Meyer J, Houle S. 2003. Synthesis and in vivo evaluation of novel radiotracers for the in vivo imaging of the norepinephrine transporter. Nucl Med Biol 30:85–92.